

Charge transfer and screening in individual C_{60} molecules on metal substrates: A scanning tunneling spectroscopy and theoretical study

Xinghua Lu, M. Grobis, K. H. Khoo, Steven G. Louie, and M. F. Crommie

*Department of Physics, University of California at Berkeley, Berkeley, California 94720-7300, USA
and Materials Sciences Division, Lawrence Berkeley Laboratory, Berkeley, California 94720-7300, USA*
(Received 27 December 2003; revised manuscript received 28 April 2004; published 24 September 2004)

We have used scanning tunneling microscopy and spectroscopy to study the electronic structure of individual C_{60} molecules adsorbed onto the Au(111) and Ag(100) surfaces. C_{60} molecules on Au(111) show an increase in the HOMO-LUMO gap of 0.6 eV compared to C_{60} on Ag(100). Splitting of the C_{60} LUMO manifold is suppressed for C_{60} on Au(111), in contrast to the strong splitting observed for C_{60} on Ag(100). Our data implies a 0.6 eV increase in intramolecular Coulomb energy for C_{60} on Au(111) as compared to C_{60} on Ag(100). Topographs and energy-resolved spectral maps, however, show nearly identical features and indicate a similar influence of the two substrates on molecular-orbital geometry. C_{60} -substrate bonding and charge transfer is further investigated by calculating C_{60} charge redistribution using *ab initio* pseudopotential density-functional theory methods. These calculations indicate that a negligible amount of charge is transferred from Au(111) to adsorbed C_{60} , while about 0.2 electron is transferred to C_{60} resting on Ag(100), although the precise amount depends on the definition used. This charge transfer likely changes the electronic screening properties of C_{60} , providing an explanation for observed spectroscopic differences on these two substrates.

DOI: 10.1103/PhysRevB.70.115418

PACS number(s): 73.22.-f, 71.15.-m, 73.63.-b

I. INTRODUCTION

The C_{60} molecule is the most common fullerene and has been used as a basic component in a variety of new carbon nanostructures, including endohedral fullerenes,¹ peapod nanotubes,² C_{60} dimers,³ and single-molecule transistors.⁴ In addition to their flexibility as nanostructural building blocks, fullerene systems can also be electronically tuned from semiconducting to superconducting behavior via charge doping.⁵ Understanding the electronic properties of C_{60} molecules in these different environments is critical for understanding and predicting the behavior of new C_{60} -derived molecular structures and devices.

One of the most fundamental properties of C_{60} electronic structure is the energy location of the lowest unoccupied molecular-orbital (LUMO) and the highest occupied molecular-orbital (HOMO) states, both of which can be changed by substrate-induced charging effects. Charge transfer, intramolecular Coulomb energy (U), and screening effects all play an important role in determining the HOMO and LUMO level structure of adsorbed C_{60} . In general, intramolecular Coulomb repulsion changes the energy required for electrons to be either added or removed from an adsorbed molecule during a measurement, thus increasing observed HOMO-LUMO gaps by U in photoemission/inverse-photoemission and electron-tunneling experiments. Screening by a substrate, however, tends to reduce Coulomb repulsion and thus also influences the HOMO-LUMO gap seen in electron spectroscopies. In this paper we gain insight into the screened electronic structure of C_{60} molecules by performing a comparative scanning tunneling spectroscopy study of C_{60} on two surfaces having very different work functions: Au(111) and Ag(100).

C_{60} electronic structure has already been studied extensively via photoemission and inverse photoemission.⁶⁻⁹ Gas

phase C_{60} and C_{60}^- photoemission has shown a HOMO-LUMO gap of 4.9 eV for isolated C_{60} .⁷ Photoemission and inverse photoemission on C_{60} monolayers have shown a HOMO-LUMO gap of 2.1 eV, 2.2 eV, and 3.2 eV for C_{60} on Au(110), Ag(110), and Cu(111), respectively.⁶ These techniques suggest charge transfers of 0.8, 1.7, and 1.6 electrons gained per C_{60} molecule for undoped C_{60} monolayers on Au(111), Ag(100), and Cu(111), respectively.^{6,8} On *n*-type GaAs(110) substrates, charge transfer of less than 0.02 electron/molecule to C_{60} was reported.⁹ Other techniques, such as electron energy-loss spectroscopy,¹⁰ have also been used to measure the charge transfer from substrate to C_{60} monolayer, but with a relatively larger uncertainty of ± 1 electron per molecule.

Measurement of the local electronic structure of individual C_{60} molecules has also been performed via scanning tunneling microscopy and spectroscopy (STM/STS). STM/STS has the advantage that it can provide both good spatial and good spectroscopic resolution, and can also investigate both filled and empty state behavior. Previous STM studies have revealed the topographic features of C_{60} molecules adsorbed to various metal¹¹⁻¹³ and semiconducting¹⁴ surfaces. Tunneling spectra of C_{60} molecules on semiconductor,¹⁵ metal,¹⁶ and insulating layers¹⁷ have shown features attributed to HOMO and LUMO molecular states. Recently, the energy-resolved spatial distribution of molecular orbitals derived from the HOMO, LUMO, and LUMO+1 states was obtained for individual C_{60} molecules¹⁸ and C_{60} monolayers¹⁹ adsorbed onto Ag(100).

Here we present STM/STS experimental data and theoretical results obtained for individual C_{60} molecules deposited onto Au(111), and we compare these to our previous results for C_{60} on Ag(100).¹⁸ We observe distinct differences in the experimental C_{60} spectra obtained for these two substrates, the most significant of which is a 0.6 eV shift to higher

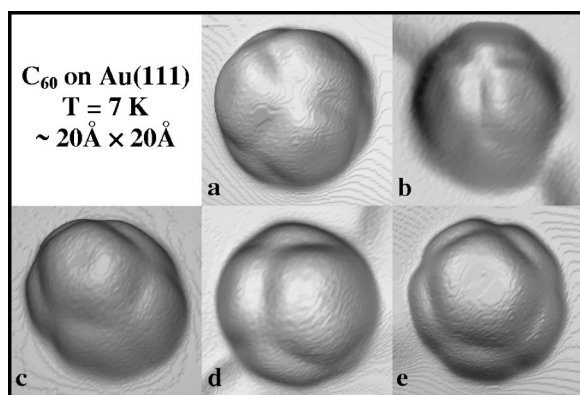


FIG. 1. Constant current topographs of individual C_{60} molecules having different orientations on the Au(111) surface at $T=7$ K ($V=2.0$ V, $I=0.3$ nA). The topmost features are (a) a hexagon ring, (b) a 6:6 bond, (c) a 5:6 bond, (d) an apex atom, and (e) a pentagon ring, respectively.

energy for C_{60} empty state peaks on Au(111), which leads to an increased HOMO-LUMO gap for C_{60} on Au versus Ag. While the leading edge of the C_{60} LUMO resonance on Ag(100) intersects the Fermi energy (E_F), the same resonance peak on Au(111) does not. In addition, we see a suppression in the experimental splitting of the C_{60} LUMO resonance on Au(111) compared to what is seen for C_{60} on Ag(100). Energy-resolved spectral density maps (in real space) of the HOMO, LUMO, and LUMO+1 derived states for C_{60} on Au(111) and Ag(100) are nearly identical despite the differences seen spectroscopically in energetic peak locations. The energy differences observed between these resonance peaks allow us to determine that the intramolecular Coulomb energy for C_{60} on Au(111) is 0.6 eV larger than for C_{60} on Ag(100). We believe that the reduced U observed for C_{60} on Ag(100) is due to increased screening arising from charge transferred to the molecule on this surface. This interpretation is bolstered by the fact that our density-functional theory (DFT) calculations show a transfer to C_{60} of about 0.2 electron per molecule on Ag(100) and a negligible amount of charge transfer for C_{60} on Au(111).

II. EXPERIMENTAL RESULTS

Our experiments were conducted using a homebuilt ultra-high vacuum (UHV) STM. The single-crystal Au(111) substrates were cleaned in UHV and dosed with C_{60} after being cooled to 7 K. dI/dV spectra were measured through lock-in detection of the ac tunneling current driven by a 450 Hz, 10 mV (rms) signal added to the junction bias under open-loop conditions (bias voltage here is defined as the sample potential referenced to the tip). dI/dV images were acquired by positioning the STM tip at each point at constant current and then measuring dI/dV . All data shown were acquired at $T=7$ K.

Figure 1 shows representative ~ 20 Å \times 20 Å topographs of C_{60} molecules on the Au(111) surface. Less than 0.01 monolayer of C_{60} was deposited onto Au(111), so the C_{60} molecules were widely separated. We found that C_{60} mol-

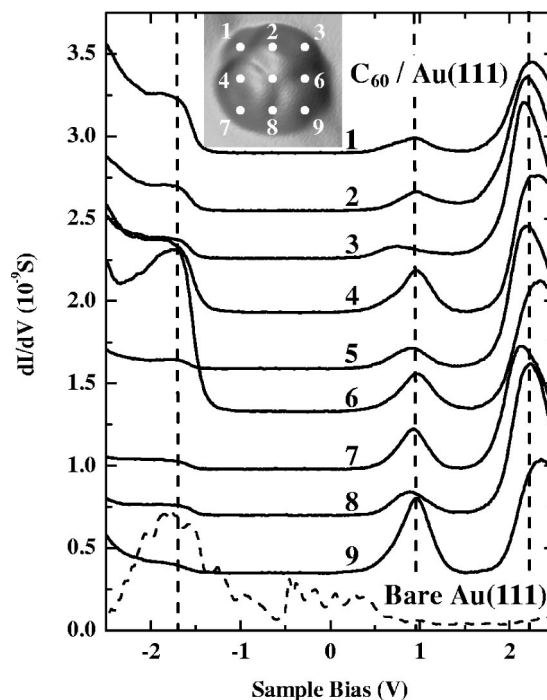


FIG. 2. dI/dV spectra of a single C_{60} molecule on Au(111) at $T=7$ K. Spectra 1–9 were taken at indicated spots on the inset image and are shifted vertically for clarity. Tunneling parameters were $V=2.0$ V, $I=1.0$ nA before taking the spectra. The dashed spectrum was obtained from the bare Au(111) surface. [Image scale is ~ 20 Å \times 20 Å.].

ecules reside both at Au step edges and on the Au terrace (terrace adsorbates were mainly found at corner sites of the herringbone reconstruction). We carefully examined ~ 90 C_{60} molecules on Au(111) using many different tips, and observed five distinct molecular orientations (shown in Fig. 1). The fivefold segments seen on the molecules arise from C_{60} pentagon rings¹⁸ and can be used to deduce the molecular orientation. The topmost features in the five orientations shown are (a) a hexagon ring, (b) a 6:6 bond (i.e., the bond separating two adjacent hexagon rings), (c) a 5:6 bond (i.e., the bond separating a pentagon ring and a hexagon ring), (d) an apex atom, and (e) a hexagon ring. These orientations were observed with an approximate distribution of 38%, 35%, 13%, 8%, and 6%, respectively. Each orientation has been observed both at step edges and at terrace sites on Au(111).

The local electronic structure of C_{60} adsorbates can be measured via differential conductance (dI/dV) spectroscopy. Figure 2 shows typical dI/dV spectra measured at nine different spots over a single C_{60} molecule adsorbed to the Au(111) surface. There are three main resonance peaks observed in the ± 2.5 V energy range, and the amplitude of these peaks varies strongly over the surface of a single molecule. Based on the measured spectra of ~ 45 molecules on Au(111), we determine that the resonances are centered at -1.7 ± 0.2 V (HOMO), 1.0 ± 0.2 V (LUMO), and 2.2 ± 0.2 V (LUMO+1). We have observed no obvious dependence of the C_{60} electronic structure on molecular orientation. Pronounced differences are observed between these

spectra and the spectra obtained for C_{60} on Ag(100) (Ref. 18) [for convenience, the $C_{60}/Ag(100)$ spectra from Ref. 18 are reproduced in Fig. 4, where they can be directly compared to the $C_{60}/Au(111)$ data]. First, the LUMO and LUMO+1 states of C_{60} on Au(111) are shifted up in energy with respect to E_F by 0.6 V. Second, there is no clear splitting of the LUMO states on Au(111), while C_{60} spectra on Ag(100) show a strong 0.4 V splitting and an enhancement of the local density of states (LDOS) in the vicinity of E_F . Third, the HOMO-LUMO gap for C_{60} on Au(111) is significantly larger than that for C_{60} on Ag(100).

The spatial inhomogeneity of the spectra observed for C_{60} arises from the LDOS distribution of the different molecular orbitals. In order to experimentally untangle the behavior of individual C_{60} molecular orbitals, one must perform energy-resolved spectroscopic mapping of the molecule. This is accomplished by spatially mapping dI/dV at a constant voltage over the molecule's surface. In the left side of Fig. 3 we present experimental energy-resolved spectroscopic maps of one C_{60} molecule taken at the energies of the three resonances observed in the spectra of C_{60} on Au(111) (all images shown in Fig. 3 were acquired with the same tip). The dI/dV map of the highest energy resonance [2.2 V, Fig. 3(b)] shows clearly resolved "bright rings," indicating LDOS buildup at the expected sites of C_{60} pentagon rings. At the 1.0 V resonance [Fig. 3(c)] we see a nearly perfect inversion of the bright ring LDOS observed at 2.2 V. The spectral map of the lowest ring LDOS observed at -1.7 V. The spectral map of the lowest energy state (-1.7 V) shows a network of LDOS peaks displaced from the high-density regions observed at other energies. In order to compare these spectral images to what is seen for C_{60} on Ag(100), we label the weak $C_{60}/Ag(100)$ resonance at E_F as $LUMO_\alpha$ and the stronger resonance at 0.4 eV as $LUMO_\beta$ [see Fig. 4(c)]. The spectral maps observed for $C_{60}/Au(111)$ in Fig. 3 are nearly identical to spectral maps previously observed for the HOMO, $LUMO_\beta$, and $LUMO+1$ resonances of C_{60} on Ag(100) [no $C_{60}/Au(111)$ resonance has a density pattern similar to that seen for $LUMO_\alpha$].¹⁸

Quantitatively determining the HOMO-LUMO gap for C_{60} on Au(111) is straightforward because the HOMO and LUMO resonances are each well-defined single peaks in the STM spectroscopic data. The energy difference between the centers of these peaks yields a HOMO-LUMO gap of 2.7 ± 0.2 eV for C_{60} adsorbed to Au(111).

Determining the corresponding HOMO-LUMO gap for C_{60} on Ag(100) is considerably more difficult because only the falling edge of the HOMO resonance is experimentally well defined for STM spectra in this system, and the LUMO resonance is split into the $LUMO_\alpha$ and $LUMO_\beta$ peaks [see spectra reproduced in Fig. 4(c)]. In order to quantitatively compare the HOMO-LUMO gap of the $C_{60}/Ag(100)$ and $C_{60}/Au(111)$ systems, we define the HOMO-LUMO gap for $C_{60}/Ag(100)$ in the following manner. We first choose the $C_{60}/Ag(100)$ $LUMO_\beta$ resonance to compare with the LUMO resonance of $C_{60}/Au(111)$. The reason for this choice is that the LUMO-LUMO+1 energy difference is the same for $C_{60}/Ag(100)$ and $C_{60}/Au(111)$ if $LUMO_\beta$ is used. Spectral maps of the $C_{60}/Ag(100)$ $LUMO_\beta$ state and the $C_{60}/Au(111)$ LUMO state also show identical density distri-

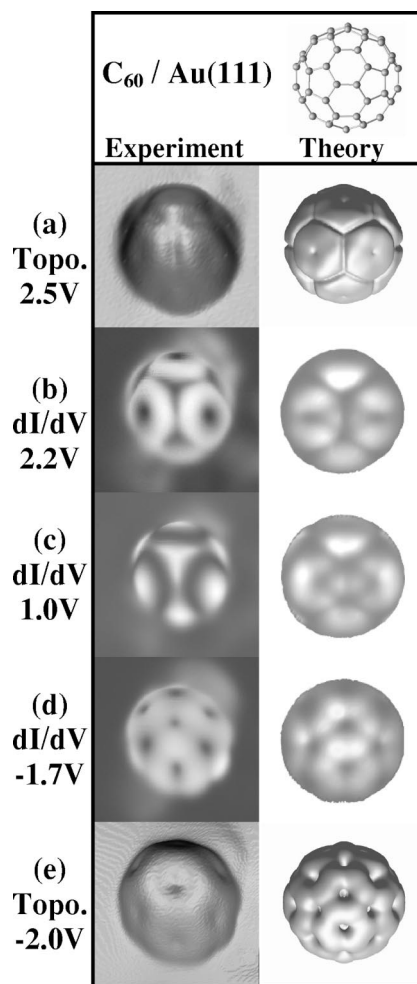


FIG. 3. Left column: experimental topographs and scanning tunneling spectroscopy images of a single C_{60} molecule. (a) Topograph taken at 2.5 V, (b)–(d) dI/dV maps taken at $V=2.2$ V, 1.0 V, and -1.7 V, (e) topograph taken at -2.0 V. Right column: simulated topographs and spectroscopic images obtained from LDA calculation. Constant current topographs are visualized as 3D rendered surfaces while spectral maps are visualized as 2D projections. [Experimental image scale: $\sim 20 \text{ \AA} \times 20 \text{ \AA}$].

butions, in contrast to what is seen for $LUMO_\alpha$. Next, the energy of the $C_{60}/Ag(100)$ HOMO resonance is determined by fitting the downward slope of the HOMO shoulder to a line and then finding the intercept of this line with the LDOS baseline. The HOMO peak center is then located below this energy by an amount equal to half the full width of the HOMO resonance. If we assume that the $C_{60}/Ag(100)$ HOMO resonance has the same width as the $C_{60}/Au(111)$ HOMO resonance, then this distance is 0.3 eV.²⁰ Such a procedure yields a HOMO-LUMO gap of 2.1 ± 0.2 eV for C_{60} on Ag(100).

III. DFT-LDA CALCULATIONS

To understand the differences in electronic structure observed for C_{60} on Au and Ag, we have carried out *ab initio* pseudopotential density-functional^{21,22} calculations. The cal-

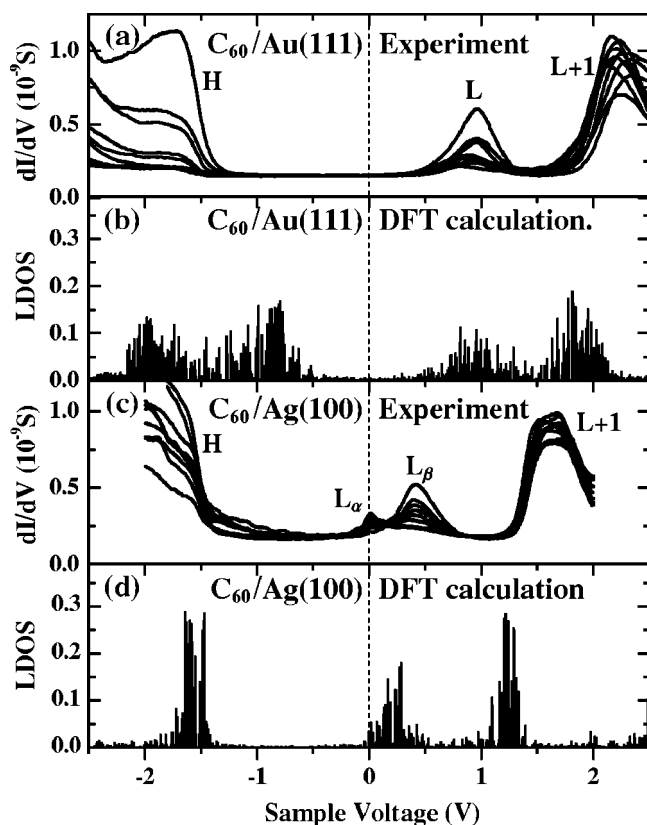


FIG. 4. Comparison of electronic structure of individual C_{60} molecules on Ag(100) and Au(111) surfaces. (a) and (c) show experimental dI/dV spectra obtained via STM spectroscopy (spectra taken at different points on the molecule are all shown together). (b) and (d) are LDOS spectra obtained via DFT calculation. HOMO (H), LUMO (L), and LUMO+1 (L+1) states are marked on the experimental spectra. The feature located at -2 V in (b) is derived from the HOMO-1 state and cannot be seen in (d) because the $C_{60}/Ag(100)$ states are shifted to lower energy.

calculations were performed with a numerical atomic-orbital basis set using the SIESTA (Ref. 23) code and the local-density approximation (LDA) was used for the exchange-correlation potential. Norm-conserving pseudopotentials were generated within the Troullier-Martins scheme.²⁴ We used a double- ζ pseudoatomic basis set of finite range consisting of s and d orbitals for Ag and Au atoms, and s and p orbitals for C atoms.²⁵ The ranges of the orbitals were determined by fixing the energy shift due to the confinement of the basis orbitals to be 0.005 Ry as described in Ref. 23. A supercell containing a C_{60} molecule and 144 surface atoms in four atomic layers was chosen for the calculation. The total energy and charge densities were calculated over a real grid with an average point spacing of about 0.3 a.u. The C_{60} molecule was positioned with a 6:6 bond directly above a substrate atom for both the Au(111) and Ag(100) calculations. The C_{60} molecule and the top layer of the substrate were allowed to relax for energy minimization. LDOS spectra were calculated at eight k points in the Brillouin zone. The effect of tip trajectory is included in the spectral maps by calculating the energy-resolved LDOS on constant total LDOS contours.¹⁸

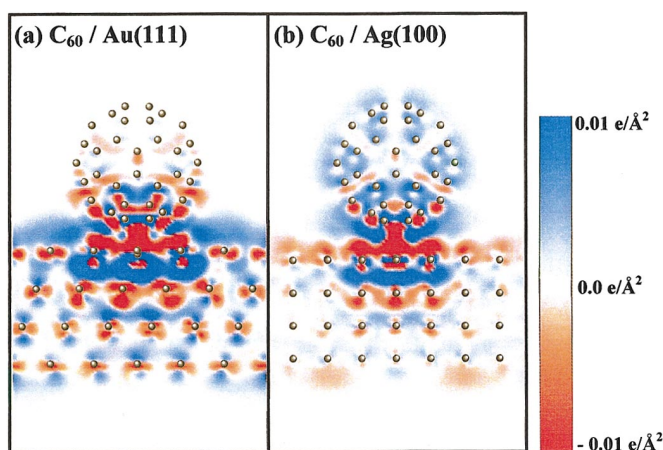


FIG. 5. (Color) Integrated differential electron density of C_{60} on (a) Au(111) and (b) Ag(100) surfaces, obtained through DFT calculation. Differential electron density is integrated along direction perpendicular to the page. Blue color represents an increase in electron density while red represents a decrease in electron density.

Figure 4(b) shows the theoretically calculated LDOS spectrum for a C_{60} molecule on Au(111). Comparison with the experimental spectra in Fig. 4(a) shows that the position and width of the theoretical LUMO resonance are well matched to the data. The theoretical LUMO-LUMO+1 energy difference for $C_{60}/Au(111)$ is similar to the experimental value, but is slightly underestimated. The theoretical HOMO-LUMO gap, however, is significantly smaller than what is seen experimentally. The $C_{60}/Ag(100)$ theoretical spectrum shown in Fig. 4(d) also does a good job of reproducing the basic energy and width of the experimental LUMO resonance for this system (the LUMO $_{\alpha}$ -LUMO $_{\beta}$ split, though, is not pronounced in the calculation). As with $C_{60}/Au(111)$, the theoretical LUMO-LUMO+1 energy difference for $C_{60}/Ag(100)$ is underestimated compared to experiment. In contrast to the $C_{60}/Au(111)$ results, however, the $C_{60}/Ag(100)$ HOMO-LUMO gap comparison is much closer for the experimental and theoretical spectra seen in Figs. 4(c) and 4(d).²⁶ It is well known that DFT-LDA calculated eigenvalues reproduce energy-level spacings well except between occupied and unoccupied states.²⁷ This is due to quasiparticle self-energy effects arising from electron-electron interactions. Our experimental and theoretical results are consistent with these expectations and also show good agreement within the limitations of the DFT method.

The calculated topographs and energy-resolved LDOS maps for C_{60} on Au(111) are presented in the right side column of Fig. 3. Many of the features in the experimental topographs and dI/dV maps are reproduced in the calculation, but the inversion seen experimentally between LUMO and LUMO+1 spectral images is not clearly reproduced.

A significant difference exists in the theoretical charge redistributions for C_{60} adsorbed on Au(111) and on Ag(100). This can be seen in Fig. 5 where we plot the calculated differential electron density for a single C_{60} molecule lying on both a Au(111) and a Ag(100) surface. This plot shows the change in electron density that occurs in the C_{60} molecule and substrate when they are brought together. The z axis is

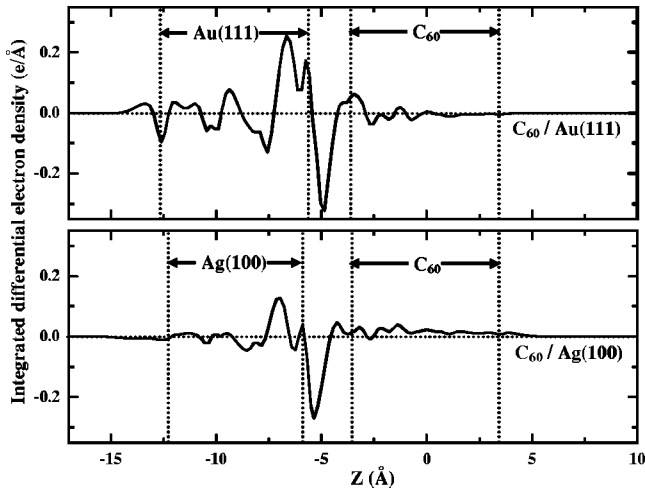


FIG. 6. Integrated differential electron density (in units of electron number/Å) of C_{60} on Au(111) and Ag(100) (positive regions have more electrons, negative regions have fewer electrons). The z axis is normal to the substrate surface and the differential electron density is integrated over the xy plane. Vertical dashed lines show the center position of atoms at the top and bottom of the metal slabs, as well as at the top and bottom of an adsorbed C_{60} molecule.

chosen to be normal to the metallic slab while the y axis is normal to the paper. The plotted differential electron density has been integrated over the y direction. The most significant deviations in electron density are seen to occur at the surface-adsorbate interface, where electrons transfer from the d -like orbitals of the substrate atoms to the p_z -like orbitals of the 6:6 carbon bond. The charge redistribution for C_{60} on Au(111) in Fig. 5(a) indicates that the primary adsorbate bonding mechanism here is *charge-neutral* polarization. For C_{60} on Ag(100), however, the charge redistribution in Fig. 5(b) shows a *net electron transfer* from the substrate to the molecule, and the adsorbate bonding mechanism is a combination of polarization and ionization.

The C_{60} charge transfer and bonding mechanisms can be seen better in Fig. 6, where we present the theoretical differential electron density integrated over the xy plane. The resulting charge redistribution for C_{60} on Au(111) shows positive and negative oscillations that average to zero, while the C_{60} molecule on Ag(100) shows a clear gain in average electron density to the molecule. To qualitatively calculate the total charge transfer, we integrate the differential electron density over the C_{60} molecule. The precise amount depends on the integration boundary. Here we define the boundary as extending from $z=+\infty$ to the plane located in the C_{60} -substrate interface region at the point where the integrated differential electron density in Fig. 6 is zero ($z \approx -4.2$ Å for $C_{60}/\text{Au}(111)$ and $z \approx -4.6$ Å for $C_{60}/\text{Ag}(100)$). This definition yields a charge transfer to the C_{60} molecule of $0.15_{-0.04}^{+0.00}$ electron for $C_{60}/\text{Ag}(100)$ and $0.01_{-0.06}^{+0.00}$ electron for $C_{60}/\text{Au}(111)$. The uncertainty in these values is calculated by redefining the C_{60} charge-transfer boundary by ± 0.5 Å. This is consistent with our experimentally measured STM spectra, which show the LUMO states of C_{60} on Au(111) to be well above E_F (and therefore empty) and the LUMO states of C_{60} on Ag(100) to be partially below E_F (and therefore partially filled).

Our charge-transfer values can be contrasted with values obtained in photoemission experiments of C_{60} monolayers on Ag(100) and Au(111) substrates, where charge transfers of 1.7 and 0.8 electrons to C_{60} are claimed,⁸ much larger values than seen here. One possible reason for this inconsistency is that photoemission experiments are done on monolayers, while here we examine isolated molecules. C_{60} monolayers and isolated C_{60} adsorbates differ in the quality of the C_{60} - C_{60} and C_{60} -substrate bonding. Our STM studies of C_{60} monolayers on Ag(100),¹⁹ however, indicate that $C_{60}/\text{Ag}(100)$ monolayers exhibit even less charge transfer than monomers, so this explanation is problematical. Though differences between PES and STS results might be caused by variations in sample preparation (such as adsorption temperature), the exact nature of the discrepancy in the charge transfer deduced from the two experiments is not well understood at this point.

IV. DISCUSSION

To understand the differences between our experimentally measured C_{60} spectra on Au and Ag substrates, we first consider the work function difference between these substrates. Because all of the molecules in this study are most likely to be in the physisorbed regime, work-function differences can be expected to play an important role in determining molecular properties. The work function of Ag(100) is 4.6 eV, 0.7 eV lower than that of Au(111).²⁸ If we assume that the electron affinity of C_{60} is not strongly changed by adsorption to Ag or Au, then we expect the LUMO state for C_{60} to lie closer to E_F for Ag than for Au by an amount approximately equal to the Au-Ag work-function difference. This provides a rough explanation as to why the C_{60} LUMO state is experimentally about 0.6 eV lower for Ag(100) than for Au(111) relative to E_F . This lowering of the C_{60} LUMO energy on Ag allows the $C_{60}/\text{Ag}(100)$ LUMO state to cross the Fermi energy and induce charge transfer to the molecule.

The Au-Ag work-function difference itself, however, is not adequate to explain the difference in HOMO-LUMO gap observed experimentally between the two substrates. We believe this arises from a difference in C_{60} charging energies for the two molecule/substrate systems. This can be understood by considering the charging energy (U) arising from Coulomb repulsion between two electrons in a C_{60} molecule. For an N -electron molecule with charging energy U , the energy of the system can be approximated as

$$E_N = \sum_{i=1}^N (\epsilon_i - \mu) + \frac{\Delta N(\Delta N - 1)}{2} U, \quad (1)$$

where $\Delta N = N - N_0$ represents the net charge of the molecule (N_0 is the number of electrons in the neutral molecule) and ϵ_i represents the mean-field molecular energy levels. Here μ represents the chemical potential of the substrate upon which the molecule is adsorbed and the summation is over all filled states. The second term represents the Coulomb energy required to charge the molecule. In a tunneling or photoemission experiment, one electron is added or removed from the molecule by providing the energy difference between the fi-

nal charged excited state and the ground state. The energy needed to add one electron to the LUMO state (labeled by $\varepsilon_{\text{LUMO}}$) of the neutral ($N=N_0$) molecule is

$$\Delta E_{+1} = E_{N_0+1} - E_{N_0} = \varepsilon_{\text{LUMO}} - \mu. \quad (2)$$

On the other hand, the energy required for removing one electron from the HOMO state (labeled by $\varepsilon_{\text{HOMO}}$) is

$$\Delta E_{-1} = E_{N_0-1} - E_{N_0} = -\varepsilon_{\text{HOMO}} + \mu + U. \quad (3)$$

The HOMO-LUMO gap seen by tunneling or photoemission can be found by adding these excitation energies:

$$\Delta E_{\text{gap}} = \Delta E_{+1} + \Delta E_{-1} = \varepsilon_{\text{LUMO}} - \varepsilon_{\text{HOMO}} + U. \quad (4)$$

The difference $\varepsilon_{\text{LUMO}} - \varepsilon_{\text{HOMO}}$ has been found from photoemission experiments to be 1.7 eV for gas phase C_{60} .⁷ Assuming that the presence of the surface does not significantly change $\varepsilon_{\text{LUMO}} - \varepsilon_{\text{HOMO}}$,¹⁸ the value of the C_{60} adsorbate charging energy can be found by subtracting 1.7 eV from our experimentally measured HOMO-LUMO gaps. This procedure leads to estimated U values of 1.0 eV for C_{60} on Au(111) and 0.4 eV for C_{60} on Ag(100). For comparison, the U value derived from photoemission results using the same procedure is 0.4 eV and 0.5 eV for $\text{C}_{60}/\text{Au}(110)$ and $\text{C}_{60}/\text{Ag}(110)$, respectively.⁶ Our STM results show a reverse trend compared to photoemission for the Ag and Au substrates, as we measure a U value for C_{60} on Au that is significantly larger than U for C_{60} on Ag.

The difference in C_{60} charging energies that we observe for Au(111) and Ag(100) is attributed to the different screening behavior induced by these two substrates. In the absence of a substrate, the value of U for isolated C_{60} has been measured to be 3.2 eV.⁷ For solid C_{60} , the value of U is reduced by half to 1.6 ± 0.2 eV, as observed by Auger spectroscopy.²⁹ Using the U values derived from our experimental spectra, screening by the Au(111) substrate is seen to reduce the C_{60} charging energy by about a factor of 3 from the isolated state, while screening by Ag(100) reduces it by a factor of 8. The relatively stronger screening for C_{60} on Ag(100) can be explained by charge transfer to the molecule on that surface. This transfer results in a net surplus of charge on the molecule at E_F , which contributes to enhanced electronic screening in C_{60} on Ag(100). Au(111), by contrast, appears to induce no such charge transfer according to our STM results and theoretical analysis. Since $\text{C}_{60}/\text{Ag}(100)$ has a higher density of states at E_F we expect it to be more polarizable and to thus behave more “metallic” than C_{60} on Au(111) [resulting in a lower charging energy for $\text{C}_{60}/\text{Ag}(100)$].

One might alternatively attribute the spectral shifts we have observed for C_{60} molecular states on Au and Ag substrates to differences in chemical bonding rather than a screened Coulomb interaction. We believe this alternative is unlikely for these physisorbed systems. This is supported by the fact that the observed LUMO-LUMO+1 energy gaps are nearly identical for C_{60} on Ag(100) and Au(111), and our energy-resolved spectral maps show nearly identical molecular-orbital features for C_{60} HOMO, LUMO, and LUMO+1 states on both substrates [assuming LUMO_β is used for $\text{C}_{60}/\text{Ag}(100)$]. If the chemical bonding details were significantly different for these two substrates then we would expect a greater variation in these properties. In addition, our LDA calculations show an absence of charge accumulation at the C_{60} -substrate interface, suggesting an absence of strong covalent bonding for both substrates. The splitting between LUMO_α and LUMO_β for $\text{C}_{60}/\text{Ag}(100)$, however, while suggested by LDA calculations,¹⁸ cannot be quantitatively explained. Jahn-Teller splitting may play a role here.³⁰

V. CONCLUSION

In conclusion, we have studied the effects of charge transfer (and the lack of it) for individual C_{60} molecules adsorbed onto Au(111) and Ag(100). We have performed spatially resolved spectroscopic measurements across individual C_{60} molecules on Au(111). We observe a HOMO-LUMO gap increase of 0.6 eV, as well as suppressed LUMO splitting, for C_{60} molecules on Au(111) compared with Ag(100). Our spectroscopic measurements allow us to infer that the C_{60} intramolecular Coulomb energy is 0.6 eV higher for C_{60} on Au(111) than for C_{60} on Ag(100). This difference is explained as the result of increased screening for C_{60} on Ag(100) relative to Au(111) due to an increase in the electronic density of states at E_F when C_{60} is adsorbed onto Ag(100). Such an interpretation is supported by LDA calculations which indicate that negligible charge is transferred from Au(111) to adsorbed C_{60} , while about 0.2 of an electron is transferred to C_{60} adsorbed onto Ag(100).

ACKNOWLEDGMENTS

This work was supported in part by NSF Grant No. DMR00-87088 and by the Director, Office of Energy Research, Office of Basic Energy Science, Division of Material Sciences and Engineering, U.S. Department of Energy under Contract No. DE-AC03-76SF0098 and Contract No. DE-AC03-76F00098. Computational resources have been provided by DOE at the National Energy Research Scientific Computing Center. The authors thank Patrick Lee and Joel Moore for helpful discussions.

¹T. Ohtsuki, K. Masumoto, K. Ohno, Y. Maruyama, Y. Kawazoe, K. Sueki, and K. Kikuchi, *Phys. Rev. Lett.* **77**, 3522 (1996); T. Ohtsuki, K. Ohno, K. Shiga, Y. Kawazoe, Y. Maruyama, and K. Masumoto, *ibid.* **81**, 967 (1998).

²B. W. Smith, M. Monthieux, and D. E. Luzzi, *Nature* (London)

396, 323 (1998); D. J. Hornbaker, S.-J. Kahng, S. Misra, B. W. Smith, A. T. Johnson, E. J. Mele, D. E. Luzzi, and A. Yazdani, *Science* **295**, 828 (2002).

³G.-W. Wang, K. Komatsu, Y. Murata, and M. Shiro, *Nature* (London) **387**, 583 (1997).

- ⁴H. Park, J. Park, A. K. L. Lim, E. H. Anderson, A. P. Alivisatos, and P. L. McEuen, *Nature (London)* **407**, 57 (2000).
- ⁵A. F. Hebard, M. J. Rosseinsky, R. C. Haddon, D. W. Murphy, S. H. Glarum, T. T. M. Palstra, A. P. Ramirez, and A. R. Kortan, *Nature (London)* **350**, 600 (1991); K. Tanigaki, T. W. Ebbesen, S. Saito, J. Mizuki, J. S. Tsai, Y. Kubo, and S. Kuroshima, *ibid.* **352**, 222 (1991); M. J. Rosseinsky, A. P. Ramirez, S. H. Glarum, D. W. Murphy, R. C. Haddon, A. F. Hebard, T. T. M. Palstra, A. R. Kortan, S. M. Zahurak, and A. V. Makhija, *Phys. Rev. Lett.* **66**, 2830 (1991).
- ⁶J. H. Weaver, *J. Phys. Chem. Solids* **53**, 1433 (1992); D. Purdie, H. Bernhoff, and B. Reihl, *Surf. Sci.* **364**, 279 (1996); K. D. Tsuei and P. D. Johnson, *Solid State Commun.* **101**, 337 (1997); K.-D. Tsuei, J.-Y. Yuh, C.-T. Tzeng, R.-Y. Chu, S.-C. Chung, and K.-L. Tsang, *Phys. Rev. B* **56**, 15412 (1997); A. J. Maxwell, P. A. Brühwiler, A. Nilsson, N. Mårtensson, and P. Rudolf, *ibid.* **49**, 10717 (1994); G. K. Wertheim and D. N. E. Buchanan, *ibid.* **50**, 11070 (1994); A. J. Maxwell, P. A. Brühwiler, D. Arvanitis, J. Hasselstrom, and N. Mårtensson, *Phys. Rev. Lett.* **79**, 1567 (1997); A. J. Maxwell, P. A. Brühwiler, D. Arvanitis, J. Hasselstrom, M. K.-J. Johansson, and N. Mårtensson, *Phys. Rev. B* **57**, 7312 (1998); K. Sakamoto, M. Harada, D. Kondo, A. Kimura, A. Kakizaki, and S. Suto, *ibid.* **58**, 13951 (1998).
- ⁷D. M. Cox, D. J. Trevor, K. C. Reichmann, and A. Kaldor, *J. Am. Chem. Soc.* **108**, 2457 (1986); S. H. Yang, C. L. Pettiette, J. Conceicao, O. Cheshnovsky, and R. E. Smalley, *Chem. Phys. Lett.* **139**, 233 (1987); A. Rosen and B. Wastberg, *J. Chem. Phys.* **90**, 2525 (1989).
- ⁸C.-T. Tzeng, W.-S. Lo, J.-Y. Yuh, R.-Y. Chu, and K.-D. Tsuei, *Phys. Rev. B* **61**, 2263 (2000); C. Cepek, M. Sancrotti, T. Greber, and J. Osterwalder, *Surf. Sci.* **454**, 467 (2000).
- ⁹T. R. Ohno, Y. Chen, S. E. Harvey, G. H. Kroll, J. H. Weaver, R. E. Haufler, and R. E. Smalley, *Phys. Rev. B* **44**, 13747 (1991).
- ¹⁰S. Modesti, S. Cerasari, and P. Rudolf, *Phys. Rev. Lett.* **71**, 2469 (1993); M. R. C. Hunt, S. Modesti, P. Rudolf, and R. E. Palmer, *Phys. Rev. B* **51**, 10039 (1995); T. Kobayashi, C. Tindall, O. Takaoka, Y. Hasegawa, and T. Sakurai, *J. Korean Phys. Soc.* **31**, S5 (1997).
- ¹¹R. Z. Bakhtizin, T. Hashizume, W. Wang, and T. Sakurai, *Phys. Usp.* **40**, 275 (1997), and references therein; T. Sakurai, X.-D. Wang, Q. K. Xue, Y. Hasegawa, T. Hashizume, and H. Shinohara, *Prog. Surf. Sci.* **51**, 263 (1996), and references therein; A. J. Maxwell, P. A. Brühwiler, S. Andersson, D. Arvanitis, B. Hernnas, O. Karis, D. C. Mancini, N. Mårtensson, S. M. Gray, M. K.-J. Johansson, and L. S. O. Johansson, *Phys. Rev. B* **52**, R5546 (1995); M. K.-J. Johansson, A. J. Maxwell, S. M. Gray, P. A. Brühwiler, and L. S. O. Johansson, *Surf. Sci.* **397**, 314 (1998); T. Hashizume, K. Motai, X. D. Wang, H. Shinohara, Y. Saito, Y. Maruyama, K. Ohno, Y. Kawazoe, Y. Nishina, H. W. Pickering, Y. Kuk, and T. Sakurai, *Phys. Rev. Lett.* **71**, 2959 (1993); Y. Maruyama, K. Ohno, and Y. Kawazoe, *Phys. Rev. B* **52**, 2070 (1995); M. T. Cuberes, R. R. Schlittler, and J. K. Gimzewski, *Appl. Phys. A: Mater. Sci. Process.* **66**, S669 (1998); P. W. Murray, I. M. Brookes, S. A. Haycock, and G. Thornton, *Phys. Rev. Lett.* **80**, 988 (1993); P. W. Murray, M. O. Pederson, E. Lægsgaard, I. Stensgaard, and F. Besenbacher, *Phys. Rev. B* **55**, 9360 (1997); J. Weckesser, J. V. Barth, and K. Kern, *ibid.* **64**, 161403 (2001); J. Weckesser, C. Cepek, R. Fasel, J. V. Barth, F. Baumberger, T. Greber, and K. Kern, *J. Chem. Phys.* **115**, 9001 (2001).
- ¹²E. I. Altman and R. J. Colton, *Phys. Rev. B* **48**, 18244 (1993); *Surf. Sci.* **295**, 13 (1993); E. Giudice, E. Magnano, S. Rusponi, C. Boragno, and U. Valbusa, *ibid.* **405**, L561 (1998); G. Costantini, S. Rusponi, E. Giudice, C. Boragno, and U. Valbusa, *Carbon* **37**, 727 (1999); C. Cepek, L. Giovannelli, M. Sancrotti, G. Costantini, C. Boragno, and U. Valbusa, *Surf. Sci.* **454**, 766 (2000); J. I. Pascual, J. Gomez-Herrero, D. Sanchez-Portal, and H.-P. Rust, *J. Chem. Phys.* **117**, 9531 (2002); W. W. Pai, C.-L. Hsu, C. R. Chiang, Y. Chang, and K. C. Lin, *Surf. Sci.* **519**, L605 (2002).
- ¹³S. Howells, T. Chen, M. Gallagher, D. Sarid, D. L. Lichtenberger, L. L. Wright, C. D. Ray, D. R. Huffman, and L. D. Lamb, *Surf. Sci.* **274**, 141 (1992); J. K. Gimzewski, S. Modesti, C. Gerber, and R. R. Schlittler, *Chem. Phys. Lett.* **213**, 401 (1993); Y. Kuk, D. K. Kim, Y. D. Suh, K. H. Park, H. P. Noh, S. J. Oh, and S. K. Kim, *Phys. Rev. Lett.* **70**, 1948 (1993); J. K. Gimzewski, S. Modesti, and R. R. Schlittler, *ibid.* **72**, 1036 (1994); C. Joachim, J. K. Gimzewski, R. R. Schlittler, and C. Chavy, *ibid.* **74**, 2102 (1995); S. Modesti, J. K. Gimzewski, and R. R. Schlittler, *Surf. Sci.* **331**, 1129 (1995); K. Sakamoto, K. Meguro, R. Arafune, M. Satoh, Y. Uehara, and S. Ushioda, *ibid.* **502**, 149 (2002); C. Rogero, J. I. Pascual, J. Gomez-Herrero, and A. M. Baro, *J. Chem. Phys.* **116**, 832 (2002); A. Marchenko and J. Cousty, *Surf. Sci.* **513**, 233 (2002).
- ¹⁴X. Yao, T. G. Ruskell, R. K. Workman, D. Sarid, and D. Chen, *Surf. Sci.* **367**, L85 (1996); P. Moriarty, Y. R. Ma, M. D. Upward, and P. H. Beton, *ibid.* **407**, 27 (1998); J. G. Hou, J. Yang, H. Wang, Q. Li, C. Zeng, H. Lin, W. Bing, D. M. Chen, and Q. Zhu, *Phys. Rev. Lett.* **83**, 3001 (1999); J. I. Pascual, J. Gomez-Herrero, C. Rogero, A. M. Baro, D. Sanchez-Portal, E. Artacho, P. Ordejon, and J. M. Soler, *Chem. Phys. Lett.* **321**, 78 (2000); J. G. Hou, J. Yang, H. Wang, Q. Li, C. Zeng, L. Yuan, B. Wang, D. M. Chen, and Q. Zhu, *Nature (London)* **409**, 304 (2001); H. Wang, C. Zeng, B. Wang, J. G. Hou, Q. Li and J. Yang, *Phys. Rev. B* **63**, 085417 (2001); L.-F. Yuan, J. Yang, H. Wang, C. Zeng, Q. Li, B. Wang, J. G. Hou, Q. Zhu, and D. M. Chen, *J. Am. Chem. Soc.* **125**, 169 (2003).
- ¹⁵T. Hashizume and T. Sakurai, *J. Vac. Sci. Technol. B* **12**, 1992 (1994); X. Yao, T. G. Ruskell, R. K. Workman, D. Sarid, and D. Chen, *Surf. Sci.* **366**, L743 (1996); H. Wang, C. Zeng, Q. Li, B. Wang, J. Yang, J. G. Hou, and Q. Zhu, *ibid.* **442**, L1024 (1999); A. W. Dunn, E. D. Svensson, and C. Dekker, *ibid.* **498**, 237 (2002).
- ¹⁶T. David, J. K. Gimzewski, D. Purdie, B. Reihl, and R. R. Schlittler, *Phys. Rev. B* **50**, 5810 (1994); M. K.-J. Johansson, A. J. Maxwell, S. M. Gray, P. A. Brühwiler, D. C. Mancini, L. S. O. Johansson, and N. Mårtensson, *ibid.* **54**, 13472 (1996).
- ¹⁷D. Porath, Y. Levi, M. Tarabiah, and O. Millo, *Phys. Rev. B* **56**, 9829 (1997).
- ¹⁸X. Lu, M. Grobis, K. H. Khoo, S. G. Louie, and M. F. Crommie, *Phys. Rev. Lett.* **90**, 096802 (2003).
- ¹⁹M. Grobis, X. Lu, and M. F. Crommie, *Phys. Rev. B* **66**, 161408 (2002).
- ²⁰The full width at half maximum of the $C_{60}/Au(111)$ HOMO resonance is 0.4 ± 0.1 eV, but the full width measured from the dI/dV base line is 0.6 eV. In order to estimate the center point of the $C_{60}/Ag(100)$ HOMO state we use half of this larger value. Use of the $C_{60}/Au(111)$ HOMO width to approximate the width of the $C_{60}/Ag(100)$ HOMO state is justified in part by the fact that the C_{60} -substrate hybridization is very similar for both phy-

- isorbed systems at 7 K (resonance widths for unoccupied C_{60} states, for example, are very similar for the two substrates). In addition, we note that photoemission measurements of C_{60}/Ag HOMO resonances yield widths that are close to the value used here (Ref. 6) (i.e., within the stated uncertainty).
- ²¹W. Kohn and L. J. Sham, *Phys. Rev.* **140**, A1133 (1965).
- ²²S. G. Louie, in *Electronic Structure, Dynamics, and Quantum Structure Properties of Condensed Matter*, edited by J. T. Devreese and P. Van Camp (Plenum, New York, 1985).
- ²³D. Sánchez-Portal, P. Ordejón, E. Artacho, and J. M. Soler, *Int. J. Quantum Chem.* **65**, 453 (1997).
- ²⁴N. Troullier and J. L. Martins, *Phys. Rev. B* **43**, 1993 (1991).
- ²⁵O. F. Sankey and D. J. Niklewski, *Phys. Rev. B* **40**, 3979 (1989).
- ²⁶The $C_{60}/Ag(100)$ spectra has been recalculated here to give a wider energy window with a higher degree of accuracy. The differences are quite minimal as compared to the calculated spectrum in Ref. 18.
- ²⁷M. S. Hybertsen and S. G. Louie, *Phys. Rev. B* **34**, 5390 (1986).
- ²⁸H. B. Michaelson, *J. Appl. Phys.* **48**, 4729 (1977); M. Uda, A. Nakamura, T. Yamamoto, and Y. Fujimoto, *J. Electron Spectrosc. Relat. Phenom.* **88**, 643 (1998).
- ²⁹R. W. Lof, M. A. van Veenendaal, B. Koopmans, H. T. Jonkman, and G. A. Sawatzky, *Phys. Rev. Lett.* **68**, 3924 (1992).
- ³⁰K. Harigaya, *Phys. Rev. B* **45**, 13676 (1992); J. Fulara, M. Jakobi, and J. P. Maier, *Chem. Phys. Lett.* **211**, 227 (1993); H. Kondo, T. Momose, and T. Shida, *ibid.* **237**, 111 (1995); O. Gunnarsson, H. Handschuh, P. S. Bechthold, B. Kessler, G. Gantefor, and W. Eberhardt, *Phys. Rev. Lett.* **74**, 1875 (1995); C. C. Chancey and M. C. M. O'Brien, *The Jahn-Teller Effect in C_{60} and Other Icosahedral Complexes* (Princeton University Press, Princeton, 1997).